Research Article

Colpitts Chaotic Oscillator Coupling with a Generalized Memristor

Ling Lu, Changdi Li, Zicheng Zhao, Bocheng Bao, and Quan Xu

School of Information Science and Engineering, Changzhou University, Changzhou 213164, China

Correspondence should be addressed to Bocheng Bao; mervinbao@126.com

By introducing a generalized memristor into a fourth-order Colpitts chaotic oscillator, a new memristive Colpitts chaotic oscillator is proposed in this paper. The generalized memristor is equivalent to a diode bridge cascaded with a first-order parallel RC filter. Chaotic attractors of the oscillator are numerically revealed from the mathematical model and experimentally captured from the physical circuit. The dynamics of the memristive Colpitts chaotic oscillator is investigated both theoretically and numerically, from which it can be found that the oscillator has a unique equilibrium point and displays complex nonlinear phenomena.

1. Introduction

Memristor, regarded as a fourth circuit element, is a passive two-terminal electronic element characterized by nonlinear constitutive relation of charge and flux [1, 2]. Due to the nonlinearity, memristor-based application circuits can easily generate chaotic signals, which immensely inspire research interests in the designs of various memristive chaotic circuits. In recent years, memristor-based chaotic circuits, most of all memristive Chua's chaotic circuits, have broadly been studied [3–10]. By substituting the nonlinear resistance elements, Chua's diodes, in various kinds of Chua's chaotic circuits, including classical Chua's circuit [3–8], canonical Chua's circuit [9–11], and modified Chua's circuit [12, 13], with memristors of different nonlinearities [4, 7, 12], a wide class of memristive Chua's chaotic circuits are presented and some novel features of initial state dependent dynamical behaviors are reported [3, 5, 10, 11]. However, no research literature related to memristor-based Colpitts chaotic oscillator can be found so far.

The third-order or fourth-order Colpitts oscillator is a single-transistor implementation of a sinusoidal oscillation circuit widely used in electronic circuits and communication systems [14, 15]. The operation frequency can vary from a few hertz up to the microwave region (gigahertz), depending on the making technology. The system possesses an intrinsic nonlinearity given by the exponential [14] or piece-wise linear [15] characteristic of the active device. The Colpitts oscillator can exhibit rich dynamical behaviors like many other oscillator configurations analyzed in the literatures. In particular, for the Colpitts oscillator there are extensive numerical and experimental evidences of nonlinear behaviors [14, 15]. Therefore, by introducing a memristor into the fourth-order Colpitts oscillator [15], a novel memristive Colpitts oscillator maintaining with the original advantages can easily be constructed.

An analogue memristor model can be realized by using a light-dependent resistor (LDR) circuit [16, 17]. In the same way, a simple analogue memristor model can be implemented by utilizing a diode bridge circuit [18, 19]. In this paper, a first-order generalized memristor consisting of a diode bridge cascaded with a first-order parallel RC filter [18] is utilized to implement the proposed memristive Colpitts oscillator, which is simplified from a second-order generalized memristor realized by a memristive diode bridge with LCR filter [19]. The first-order generalized memristor is composed of only elementary electronic circuit elements and is well suitable for experimental measurements. Based on the proposed memristive Colpitts chaotic oscillator, dynamical modeling, numerical simulations, and experimental observations are performed in order.
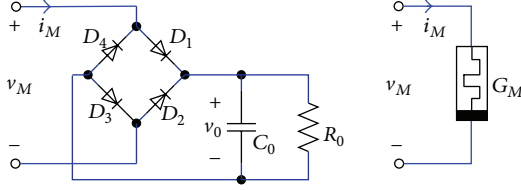
FIGURE 1: Generalized memristor realized by a diode bridge with parallel RC filter.

2. Memristive Colpitts Chaotic Oscillator

2.1. Generalized Memristor. The equivalent realization circuit of the first-order generalized memristor in [18] is shown in Figure 1, which is realized by a diode bridge cascaded with a first-order parallel RC filter. The key mechanisms at the origin of its memristive behavior are the voltage constraints involving each pair of parallel diodes [19].

Assuming that v_M and i_M represent the voltage across and the current flowing through the input terminal of the generalized memristor and v_0 is the voltage of the capacitor C_0, the mathematical model can be expressed as

$$i_M = G_M v_M = 2I_{S1}e^{-\rho_1 v_0}\sinh\left(\rho_1 v_M\right), \tag{1}$$

$$\frac{dv_0}{dt} = \frac{2I_{S1}e^{-\rho_1 v_0}\cosh\left(\rho_1 v_M\right)}{C_0} - \frac{v_0}{R_0 C_0} - \frac{2I_{S1}}{C_0}, \tag{2}$$

where $\rho_1 = 1/(2n_1 V_T)$ and I_{S1}, n_1, and V_T are the reverse saturation current, emission coefficient, and thermal voltage of the diode, respectively. In this paper, four 1N4148 diodes are utilized in Figure 1 and the diode parameters are determined by $I_{S1} = 5.84\,\mathrm{nA}$, $n_1 = 1.94$, and $V_T = 25\,\mathrm{mV}$.

The mathematical model described by (1) and (2) accords with the defining equations for the class of generalized memristors [20]. The generalized memristor is indeed voltage-controlled and its memductance is expressed as

$$G_M = \frac{2I_{S1}e^{-\rho_1 v_0}\sinh\left(\rho_1 v_M\right)}{v_M}. \tag{3}$$

Consider that the circuit parameters in Figure 1 are $R_0 = 200\,\Omega$ and $C_0 = 2\,\mu\mathrm{F}$ and the applied voltage is a bipolar sinusoidal voltage of $v_M = V_m\sin(2\pi ft)\,\mathrm{V}$. When $V_m = 2\,\mathrm{V}$ and f is set to $1\,\mathrm{kHz}$ and to $5\,\mathrm{kHz}$, respectively, the generalized memristor can display hysteresis loops pinched at the origin, as shown in Figure 2(a). It can be seen that the area of the pinched hysteresis lobe decreases monotonically as the frequency of the periodic input voltage increases and the pinched hysteresis loop shrinks to a nonlinear single-valued function when the frequency tends to infinity. Therefore, the generalized memristor can exhibit three characteristic fingerprints for identifying memristors [21]. When $f = 1\,\mathrm{kHz}$ and two voltages of $v_M = 2\sin(2\pi ft) + 1.2\cos(5\pi ft)\,\mathrm{V}$ and $v_M = 2.5 + 1.5\sin(2\pi ft)\,\mathrm{V}$ are applied, the loci in the $v_M - i_M$ plane are shown in Figure 2(b), where, for the applied voltage with the two different frequencies, the locus is a double-loop hysteresis pinched at the origin; however, for

the applied voltage with unipolarity, the locus is a single-loop hysteresis and is not pinched at the origin. Thus, for different voltage stimuli, the loci of the generalized memristor are the hysteresis loops with different shapes.

For the generalized memristor shown in Figure 1, it is remarkable that

(1) the pinched hysteresis loop is independent of the initial condition of the inner state variable v_0,

(2) the effective operating frequency range depends on the inner circuit parameters, that is, the time constant $R_0 C_0$, and will be higher for the smaller time constant,

(3) the smaller resistance R_0 can generate the bigger current i_M flowing through the generalized memristor.

2.2. Memristive Colpitts Chaotic Oscillator. It was reported in [15] that a fourth-order Colpitts oscillator can generate chaos. When a generalized memristor is introduced into the Colpitts oscillator, a novel memristor-based chaotic circuit is easily designed, as shown in Figure 3, in which the generalized memristor represents the memristive diode bridge circuit shown in Figure 1. Considering the inner state variable v_0 in the generalized memristor, the memristive Colpitts oscillator is a fifth-order circuit.

An NPN bipolar junction transistor is included as a nonlinear element in the Colpitts oscillator. When parasitic dynamics of the transistor are neglected, an intrinsic nonlinearity given by the exponential characteristic is considered to model for the active device and the common-base forward short-circuit current gain equals 1. Two parameters I_{S2} and V_T are used for the descriptions of the transport saturation current and thermal voltage of the transistor Q, respectively. For the transistor Q, the mathematical model is featured by [14]

$$i_e = I_{S2}\left(e^{v_{be}/V_T} - 1\right) = I_{S2}\left(e^{\rho_2 v_1} - 1\right), \tag{4}$$

where $\rho_2 = 1/V_T$ and i_e is the emitter current of the transistor. When the type of 2N2222 is considered in Figure 2, the transistor parameters are determined by $I_{S2} = 3.0484\,\mathrm{nA}$ and $V_T = 25\,\mathrm{mV}$.

There are four state variables of the capacitor C_1 voltage v_1, the capacitor C_2 voltage v_2, the capacitor C_3 voltage v_3, and the inductor L current i_L in the fourth-order Colpitts oscillator and one state variable of the capacitor C_0 voltage v_0 in the generalized memristor. Applying Kirchhoff's circuit laws and the constitutive relations of circuit elements, a state equation set can be obtained as

$$C_1\frac{dv_1}{dt} = i_M - i_R - \frac{V_{EE} + v_1}{R_2},$$

$$C_2\frac{dv_2}{dt} = i_R - i_M - i_e,$$

$$C_3\frac{dv_3}{dt} = i_R - i_M - i_L, \tag{5}$$

$$L\frac{di_L}{dt} = v_3,$$

$$C_0\frac{dv_0}{dt} = 2I_{S1}e^{-\rho_1 v_0}\cosh\left(\rho_1 v_M\right) - 2I_{S1} - \frac{v_0}{R_0},$$
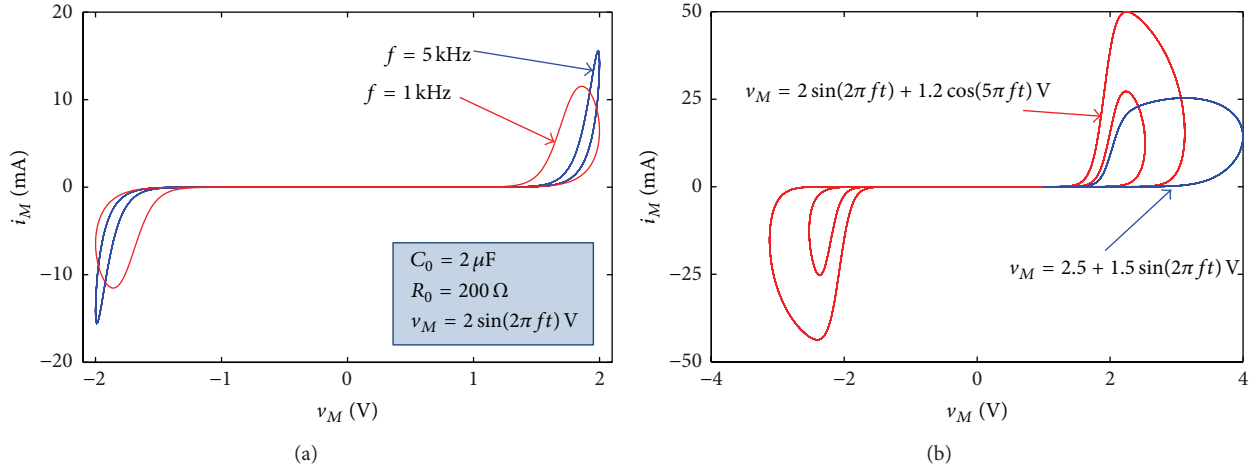
FIGURE 2: Loci in the $v_M - i_M$ plane of the generalized memristor driven by different input voltages: (a) bipolar sinusoidal voltage stimuli; (b) other periodic voltage stimuli.

where $i_b = 0$ and $i_c = i_e$ are considered, and

$$
\begin{aligned}
v_M &= -v_1 + v_2 + v_3, \\
i_M &= 2I_{S1}e^{-\rho_1 v_0}\sinh\left(\rho_1 v_M\right), \\
i_R &= \frac{\left(V_{CC} - v_M\right)}{R_1}.
\end{aligned}
\tag{6}
$$

Substituting (4) and (6) into (5) yields

$$
\begin{aligned}
\frac{dv_1}{dt} &= \frac{2I_{S1}e^{-\rho_1 v_0}\sinh\left(\rho_1 v_M\right)}{C_1} - \frac{V_{CC} - v_M}{R_1 C_1} - \frac{V_{EE} + v_1}{R_2 C_1}, \\
\frac{dv_2}{dt} &= \frac{V_{CC} - v_M}{R_1 C_2} - \frac{2I_{S1}e^{-\rho_1 v_0}\sinh\left(\rho_1 v_M\right)}{C_2} - \frac{I_{S2}\left(e^{\rho_2 v_1} - 1\right)}{C_2}, \\
\frac{dv_3}{dt} &= \frac{V_{CC} - v_M}{R_1 C_3} - \frac{2I_{S1}e^{-\rho_1 v_0}\sinh\left(\rho_1 v_M\right)}{C_3} - \frac{i_L}{C_3}, \\
\frac{di_L}{dt} &= \frac{v_3}{L}, \\
\frac{dv_0}{dt} &= \frac{2I_{S1}e^{-\rho_1 v_0}\cosh\left(\rho_1 v_M\right)}{C_0} - \frac{v_0}{R_0 C_0} - \frac{2I_{S1}}{C_0}.
\end{aligned}
\tag{7}
$$

Equation (7) is a five-dimensional nonlinear system, upon which dynamical analysis of the memristive Colpitts oscillator can be performed numerically.

3. Dissipativity and Stability Analysis

3.1. Dissipativity.
The memristive Colpitts oscillator in Figure 3 is dissipative. The dissipativity can be derived from

$$
\begin{aligned}
\nabla V &= \frac{\partial \dot{v}_1}{\partial v_1} + \frac{\partial \dot{v}_2}{\partial v_2} + \frac{\partial \dot{v}_3}{\partial v_3} + \frac{\partial \dot{i}_L}{\partial i_L} + \frac{\partial \dot{v}_0}{\partial v_0} \\
&= -2\rho_1 I_{S1}e^{-\rho_1 v_0}\cosh\left(\rho_1 v_M\right)\left(\frac{1}{C_1} + \frac{1}{C_2} + \frac{1}{C_3} + \frac{1}{C_0}\right) \\
&\quad - \frac{1}{R_1}\left(\frac{1}{C_1} + \frac{1}{C_2} + \frac{1}{C_3}\right) - \frac{1}{R_2 C_1} - \frac{1}{R_0 C_0}.
\end{aligned}
\tag{8}
$$

Considering that the hyperbolic cosine function is positive, (8) can be simplified as

$$
\nabla V < -\frac{1}{R_1}\left(\frac{1}{C_1} + \frac{1}{C_2} + \frac{1}{C_3}\right) - \frac{1}{R_2 C_1} - \frac{1}{R_0 C_0} < 0. \tag{9}
$$

Therefore, the dissipativity is always negative, implying that all orbits are ultimately confined to a specific subset of zero volume, and the asymptotic motion settles onto an attractor.

3.2. Equilibrium Point and Its Stability.
The equilibrium point of (7) is yielded by solving the following equations:

$$
R_1 R_2 i_M - R_2\left(V_{CC} - v_M\right) - R_1\left(V_{EE} + v_1\right) = 0, \tag{10a}
$$

$$
V_{CC} - v_M - R_1 i_M - R_1 I_{S2}\left(e^{\rho_2 v_1} - 1\right) = 0, \tag{10b}
$$

$$
V_{CC} - v_M - R_1 i_M - R_1 i_L = 0, \tag{10c}
$$

$$
v_3 = 0, \tag{10d}
$$

$$
2R_0 I_{S1}e^{-\rho_1 v_0}\cosh\left(\rho_1 v_M\right) - v_0 - 2R_0 I_{S1} = 0. \tag{10e}
$$

From (10b) and (10e), we obtain

$$
v_1 = \frac{1}{\rho_2}\ln\left(\frac{V_{CC} - v_M - R_1 i_M}{R_1 I_{S2}} + 1\right), \tag{11a}
$$

$$
v_M = \frac{1}{\rho_1}\operatorname{arccosh}\left[\left(\frac{v_0}{2R_0 I_{S1}} + 1\right)e^{\rho_1 v_0}\right]. \tag{11b}
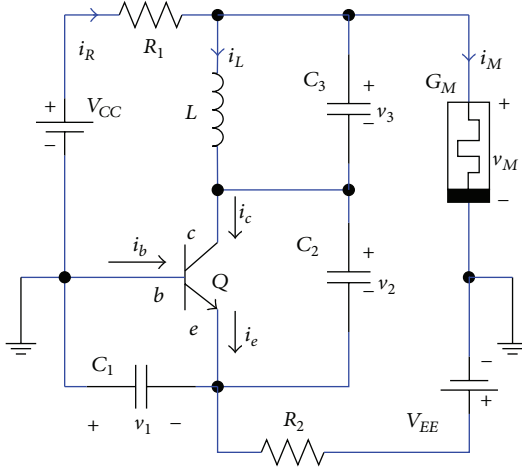$$

FIGURE 3: Memristive Colpitts chaotic oscillator based on the generalized memristor.

According to (10a), let

$$h_1 = R_1 R_2 i_M - R_2 (V_{CC} - v_M), \tag{12a}$$

$$h_2 = R_1 (V_{EE} + v_1)$$
$$= R_1 V_{EE} + \frac{R_1}{\rho_2} \ln \left(\frac{V_{CC} - v_M - R_1 i_M}{R_1 I_{S2}} + 1 \right). \tag{12b}$$

Substituting (11a) and (11b) into (12a) and (12b) and considering the voltage-current relationship of (1), it can be found that h_1 and h_2 are two functions related to v_0. Letting $h_1 = h_2$, the intersection point of two function curves described by (12a) and (12b) corresponds to the value of v_0, which represents the location of the equilibrium point on the v_0-axis and can be obtained through graphic analytic method. Then, the corresponding values of other variables can easily be calculated. For the circuit parameters listed in Table 1, the unique equilibrium point is expressed as

$$S = (0.3458, 4.7217, 0, 0.0031, 2.9460). \tag{13}$$

Observed from (10a)–(10e) it can be known that the value of the equilibrium point is mainly determined by the specified circuit parameters of R_0, R_1, and R_2. This feature is completely different from the conventional memristive chaotic circuits [3, 5, 10], whose equilibrium points are an equilibrium point set located on the axis corresponding to the inner state variable of the memristor.

The Jacobian matrix of (7), evaluated at the equilibrium point $\bar{S} = (\bar{v}_1, \bar{v}_2, \bar{v}_3, \bar{i}_L, \bar{v}_0)$, is given by

$$\mathbf{J} = \begin{bmatrix} -\dfrac{a_1}{C_1} - \dfrac{1}{R_2 C_1} & \dfrac{a_1}{C_1} & \dfrac{a_1}{C_1} & 0 & -\dfrac{a_2}{C_1} \\[2mm] \dfrac{a_1}{C_2} - \dfrac{a_3}{C_2} & -\dfrac{a_1}{C_2} & -\dfrac{a_1}{C_2} & 0 & \dfrac{a_2}{C_2} \\[2mm] \dfrac{a_1}{C_3} & -\dfrac{a_1}{C_3} & -\dfrac{a_1}{C_3} & -\dfrac{1}{C_3} & \dfrac{a_2}{C_3} \\[2mm] 0 & 0 & \dfrac{1}{L} & 0 & 0 \\[2mm] -\dfrac{a_2}{C_0} & \dfrac{a_2}{C_0} & \dfrac{a_2}{C_0} & 0 & \dfrac{1}{C_0}\left(\dfrac{1}{R_1} - \dfrac{1}{R_0} - a_1\right) \end{bmatrix}, \tag{14}$$

TABLE 1: Circuit parameters for simulations and experiments.

Parameters	Significations	Values
C_0, C_1, C_2	Capacitance	$2\,\mu\text{F}$
C_3	Capacitance	$33\,\text{nF}$
L	Inductance	$10\,\text{mH}$
R_0	Resistance	$200\,\Omega$
R_1	Resistance	$35\,\Omega$
R_2	Resistance	$1.5\,\text{k}\Omega$
V_{CC}	Direct voltage	$5\,\text{V}$
V_{EE}	Direct voltage	$-5\,\text{V}$

where

$$a_1 = 2\rho_1 I_{S1} e^{-\rho_1 \bar{v}_0} \cosh \left[\rho_1 \left(-\bar{v}_1 + \bar{v}_2 + \bar{v}_3 \right) \right] + \frac{1}{R_1},$$

$$a_2 = 2\rho_1 I_{S1} e^{-\rho_1 \bar{v}_0} \sinh \left[\rho_1 \left(-\bar{v}_1 + \bar{v}_2 + \bar{v}_3 \right) \right], \tag{15}$$

$$a_3 = \rho_2 I_{S2} e^{\rho_2 \bar{v}_1}.$$

Thus, the corresponding characteristic equation can be written as

$$\det (\mathbf{1}\lambda - \mathbf{J}) = 0. \tag{16}$$

For the circuit parameters listed in Table 1, the five eigenvalues at the equilibrium point are calculated as

$$\lambda_{1,2} = 5036 \pm j14554,$$

$$\lambda_{3,4} = -13124 \pm j3264, \tag{17}$$

$$\lambda_5 = -5710503.$$

It is found that the memristive Colpitts oscillator in Figure 3 has two complex conjugate roots with positive real parts, two complex conjugate roots with negative real parts, and one negative real root; the equilibrium point consequently is an unstable saddle-focus, resulting in the generation of the spiral chaotic attractor.

4. Typical Chaotic Attractor

In Figures 1 and 3, the circuit element parameters are listed in Table 1; the four 1N4148 diodes and the 2N2222 transistor are utilized.

4.1. Numerical Simulations. When the initial values of five state variables are selected as $v_1(0) = 0.01$ V, $v_2(0) = 0.01$ V, $v_3(0) = 0$ V, $i_L(0) = 0$ A, and $v_0(0) = 0$ V, the memristive Colpitts oscillator in Figure 3 is chaotic and displays a spiral chaotic attractor, as plotted in Figure 4. The five Lyapunov exponents are $\text{LE}_1 = 769.9443$, $\text{LE}_2 = -0.147$, $\text{LE}_3 = -3291.8$, $\text{LE}_4 = -13589$, and $\text{LE}_5 = -184610$,
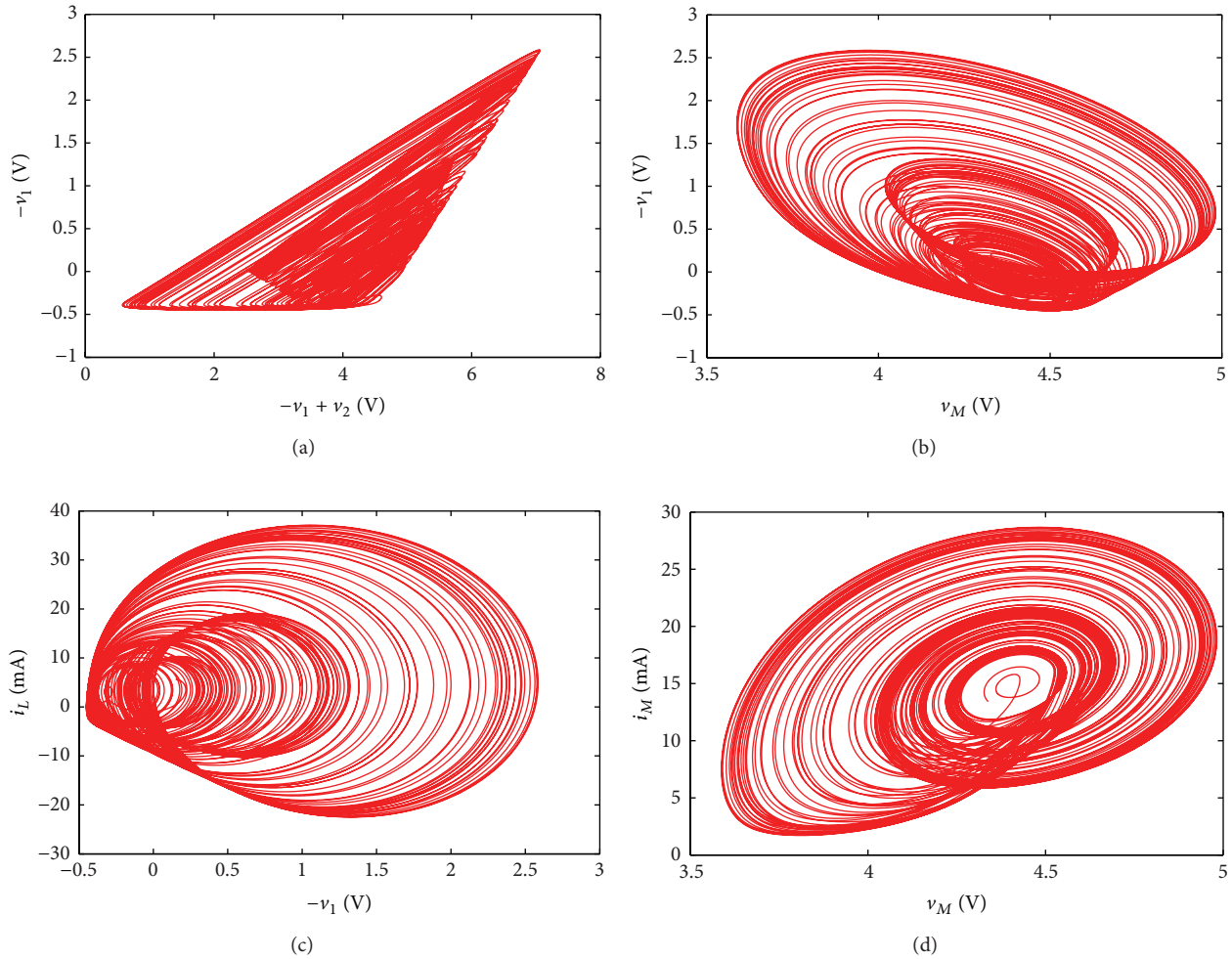
FIGURE 4: Phase portraits of the memristive Colpitts oscillator by numerical simulations: (a) $-v_1 + v_2$ versus $-v_1$; (b) v_M versus $-v_1$; (c) $-v_1$ versus i_L; (d) v_M versus i_M.

respectively. Note that Figure 4(d) displays the fingerprint of the generalized memristor, which illustrates that there exists a single-loop hysteresis behavior in the generalized memristor due to the applied positive offset voltage with unipolarity.

For the corresponding parameters, the Poincaré mappings on $v_3(t) = 0$ V section are shown in Figures 5(a) and 5(b) and the partial time-domain waveforms of the variables $v_1(t)$, $v_2(t)$, $i_M(t)$, and $v_M(t)$ are plotted in Figures 5(c) and 5(d). Observed from Figure 5, some folded sheets of the chaotic attractor are visualized and the aperiodic waveforms of the variables are captured. Therefore, the memristive Colpitts oscillator is chaotic, in which complex nonlinear phenomena can easily be observed.

4.2. Experimental Verifications. An experimental setup of the memristive Colpitts oscillator is designed to investigate the dynamical behaviors with the same circuit parameters as for numerical simulations. The chaotic behaviors of the memristive Colpitts oscillator in different phase planes can be experimentally captured in Figure 6. The experimental results in Figure 6 are consistent with the numerical simulations

and illustrate that the physical circuit can indeed generate chaos.

5. Dynamics Depending on Circuit Parameters

When the resistance R_2 is a varying parameter, the bifurcation diagram of the state variable $v_1(t)$ and the corresponding Lyapunov exponent spectra of the memristive Colpitts chaotic oscillator are depicted in Figures 7(a) and 7(b), respectively. For clarity, the first three Lyapunov exponents are presented.

As R_2 increases gradually within the parameter variation range, the dynamics of the memristive Colpitts chaotic oscillator starts from periodic behaviors and then enters into chaotic behaviors via forward period-doubling bifurcation route and finally settles down periodic behaviors via reverse period-doubling bifurcation route. Correspondingly, the maximum Lyapunov exponent begins with negative region and then reaches positive region and finally returns to negative region. Clearly, several windows of periodicities exist in the band of chaotic behaviors.
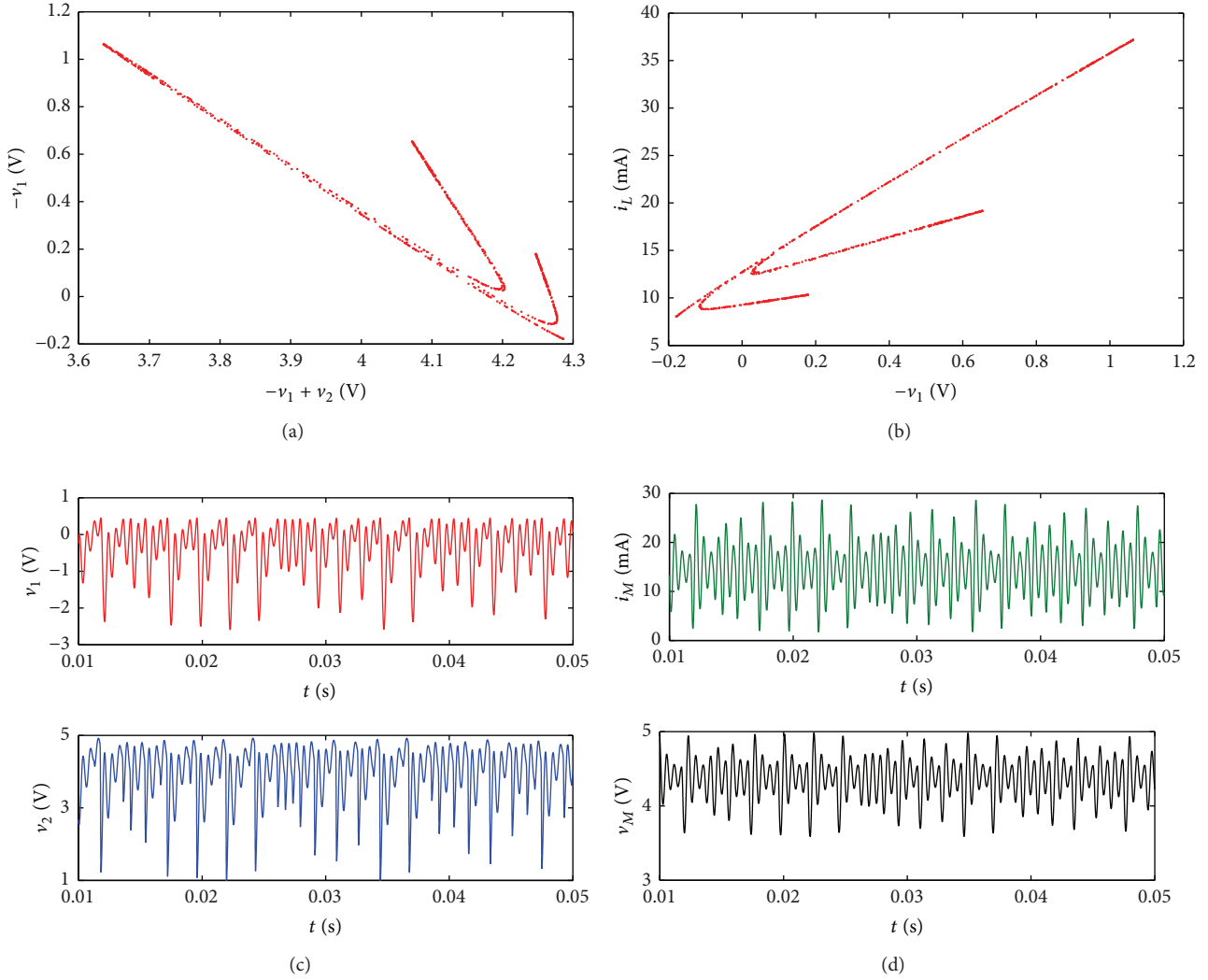
(a)

(b)

(c)

(d)

FIGURE 5: Poincaré mappings and time-domain waveforms: (a) Poincaré mapping in the $-v_1 + v_2$ and $-v_1$ plane; (b) Poincaré mapping in the $-v_1$ and i_L plane; (c) waveforms of $v_1(t)$ and $v_2(t)$; (d) waveforms of $i_M(t)$ and $v_M(t)$.

By numerical simulations, some typical chaotic and periodic orbits of the memristive Colpitts chaotic oscillator are obtained as shown in Figure 8. Figures 8(a) and 8(c) display two typical portrait phases in different chaotic regions, Figure 8(b) illustrates a typical limit cycle within periodic window, and Figure 8(d) demonstrates a normal orbit of period-2.

When the inner parameter R_0 of the generalized memristor is regarded as a bifurcation parameter, the bifurcation diagram of the state variable $v_1(t)$ and the corresponding Lyapunov exponent spectra of the memristive Colpitts oscillator are plotted in Figures 9(a) and 9(b), respectively. From Figure 9, it can be observed that, except for two periodic windows, chaotic behavior appearing in the memristive Colpitts oscillator has good robustness. Correspondingly, two typical portrait phases in the $v_M - i_M$ plane are shown in Figure 10, which demonstrate that the generalized memristor

only exhibits positive right part of pinched hysteresis loops due to the applied positive stimuli.

6. Conclusions

In this paper, a novel memristive Colpitts chaotic oscillator is presented, which is derived from a fourth-order Colpitts chaotic oscillator coupling with a generalized memristor. The generalized memristor is equivalently realized by a diode bridge cascaded with a first-order parallel RC filter and its fingerprints of the pinched hysteresis loops are further elaborated. Theoretical analyses, numerical simulations, and experimental measurements of the memristive Colpitts chaotic oscillator are performed in order. The dynamical investigations indicate that the oscillator only has an unstable equilibrium point and displays complex nonlinear phenomena. The memristive Colpitts chaotic oscillator is simple and easy to implement physically, which can be used to generate chaotic signals for various engineering applications.
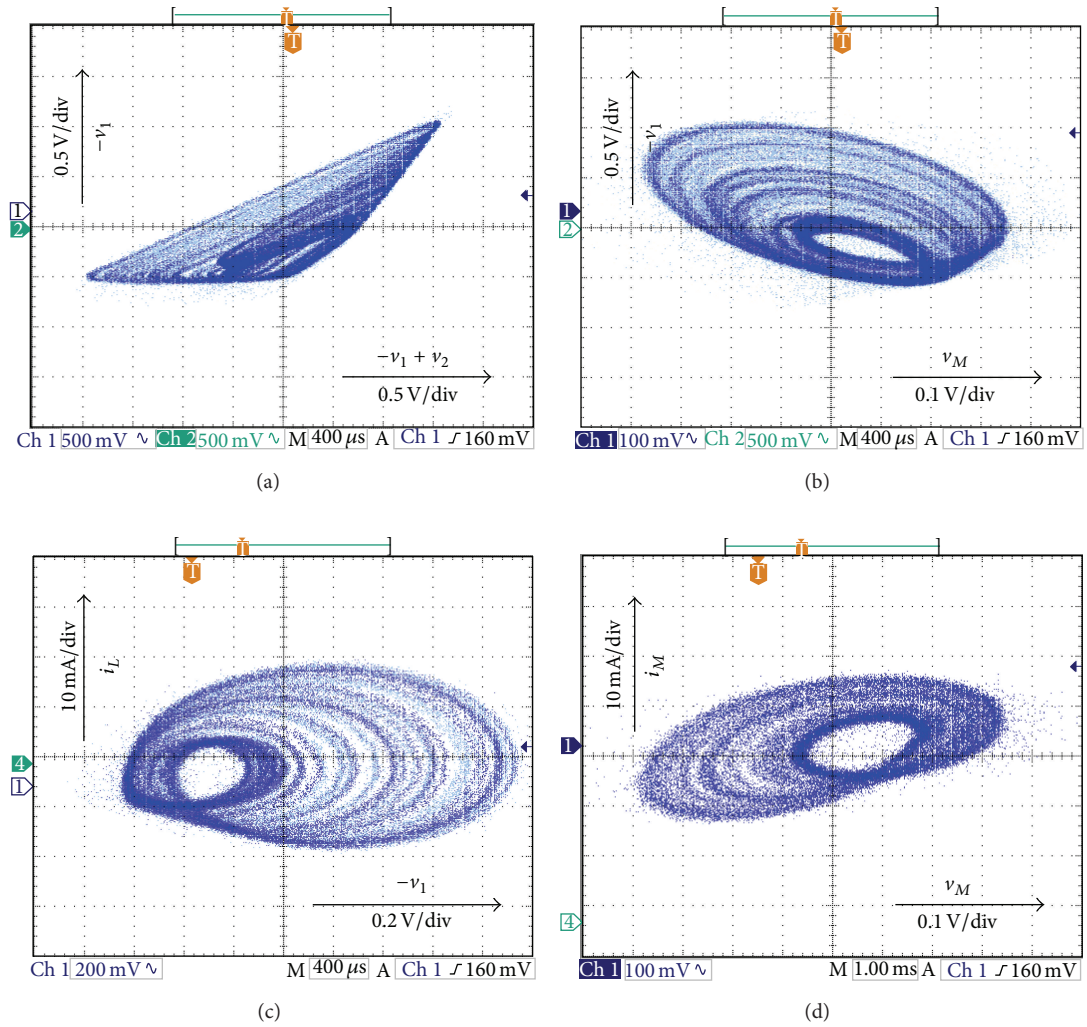
Figure 6: Phase portraits of the memristive Colpitts oscillator by experimental measurements: (a) $-v_1 + v_2$ versus $-v_1$; (b) v_M versus $-v_1$; (c) $-v_1$ versus i_L; (d) v_M versus i_M.
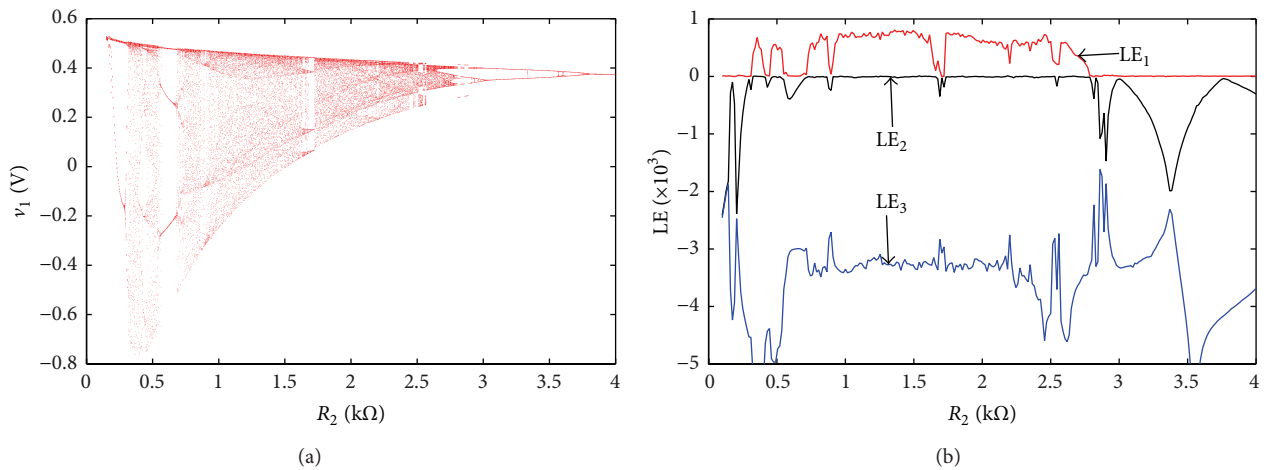

Figure 7: Dynamics with the resistance R_2 increasing: (a) bifurcation behavior of $v_1(t)$; (b) Lyapunov exponent spectra.
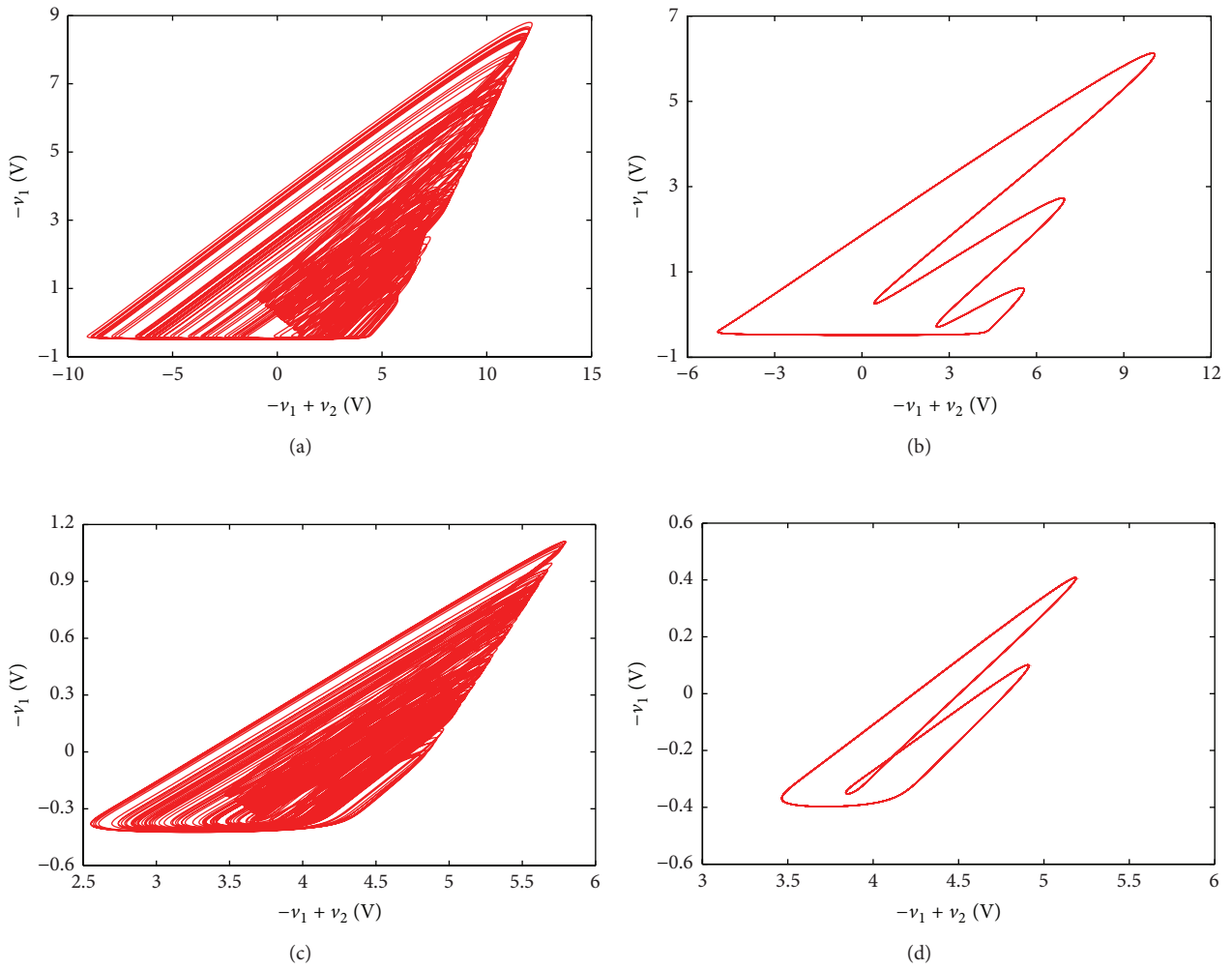
(a)

(b)

(c)

(d)

FIGURE 8: Chaotic and periodic orbits in the $-v_1 + v_2$ and $-v_1$ plane: (a) chaotic attractor ($R_2 = 0.5\,k\Omega$); (b) period-3 limit cycle with ($R_2 = 0.6\,k\Omega$); (c) chaotic attractor ($R_2 = 2.4\,k\Omega$); (d) limit cycle with period-2 ($R_2 = 3.1\,k\Omega$).
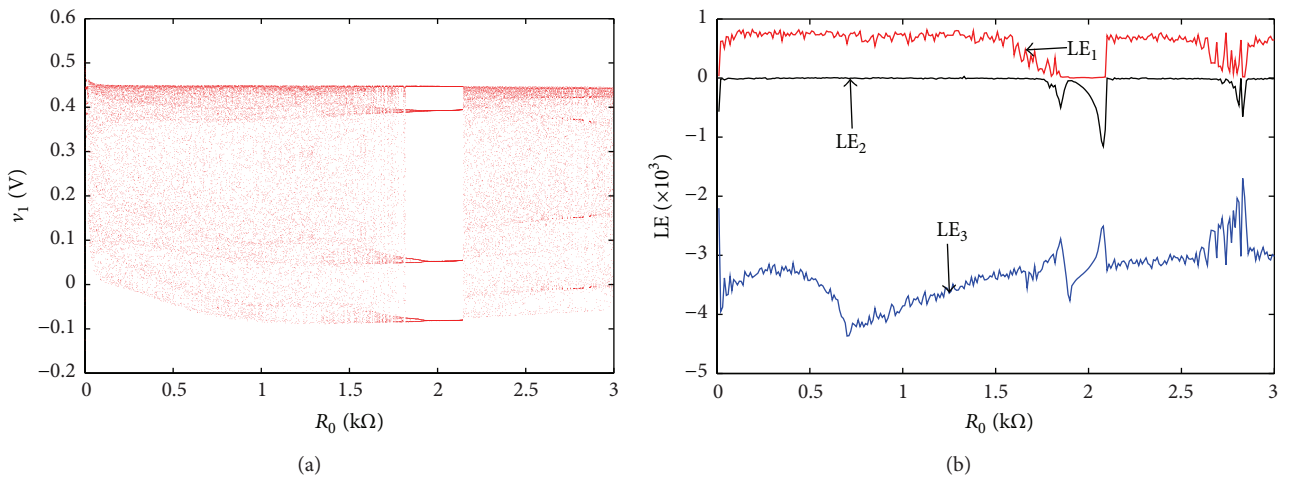

(a)

(b)

FIGURE 9: Dynamics with the resistance R_0 increasing: (a) bifurcation behavior of $v_1(t)$; (b) Lyapunov exponent spectra.
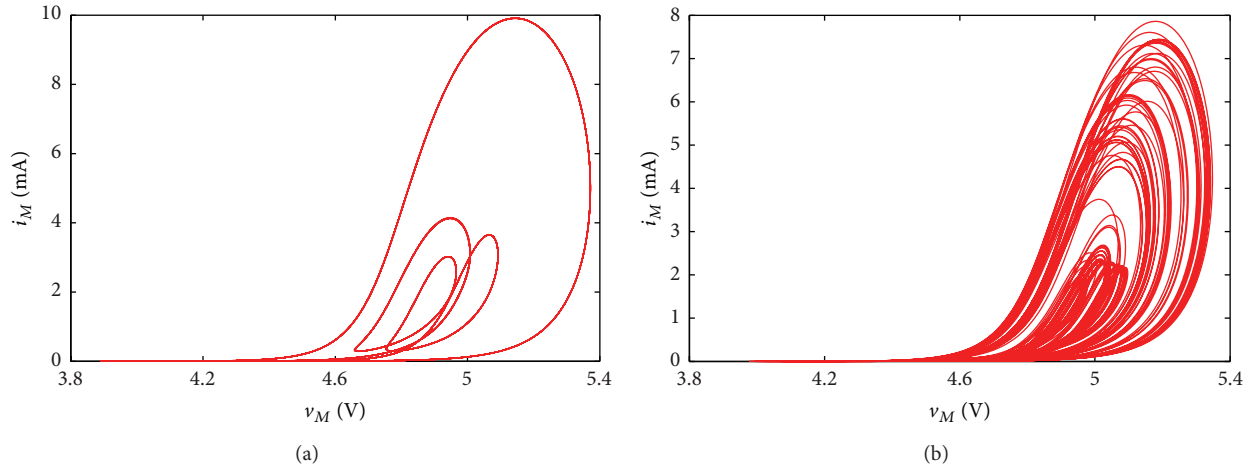
(a)

(b)

FIGURE 10: Periodic and chaotic orbits in the $v_M - i_M$ plane: (a) limit cycle with period-4 ($R_2 = 2\,\text{k}\Omega$); (b) chaotic attractor ($R_0 = 3\,\text{k}\Omega$).

Conflict of Interests

The authors declare that there is no conflict of interests regarding the publication of this paper.

Acknowledgments

References

[1] D. B. Strukov, G. S. Snider, D. R. Stewart, and R. S. Williams, "The missing memristor found," *Nature*, vol. 453, pp. 80–83, 2008.

[2] L. O. Chua, "Memrister—the missing circuit element," *IEEE Transactions on Circuit Theory*, vol. 18, no. 5, pp. 507–519, 1971.

[3] B.-C. Bao, J.-P. Xu, and Z. Liu, "Initial state dependent dynamical behaviors in a memristor based chaotic circuit," *Chinese Physics Letters*, vol. 27, no. 7, Article ID 070504, 2010.

[4] Y. Li, X. Huang, and M. Guo, "The generation, analysis, and circuit implementation of a new memristor based chaotic system," *Mathematical Problems in Engineering*, vol. 2013, Article ID 398306, 8 pages, 2013.

[5] B. Muthuswamy, "Implementing memristor based chaotic circuits," *International Journal of Bifurcation and Chaos*, vol. 20, no. 5, pp. 1335–1350, 2010.

[6] G.-Y. Wang, J.-L. He, F. Yuan, and C.-J. Peng, "Dynamical behaviors of a TiO$_2$ memristor oscillator," *Chinese Physics Letters*, vol. 30, no. 11, Article ID 110506, 2013.

[7] B.-C. Bao, J.-P. Xu, G.-H. Zhou, Z.-H. Ma, and L. Zou, "Chaotic memristive circuit: equivalent circuit realization and dynamical analysis," *Chinese Physics B*, vol. 20, no. 12, Article ID 120502, 2011.

[8] B. Bao, F. Hu, Z. Liu, and J. Xu, "Mapping equivalent approach to analysis and realization of memristor-based dynamical circuit," *Chinese Physics B*, vol. 23, no. 7, Article ID 070503, 2014.

[9] A. Buscarino, L. Fortuna, M. Frasca, and L. V. Gambuzza, "A chaotic circuit based on Hewlett-Packard memristor," *Chaos*, vol. 22, no. 2, Article ID 023136, 2012.

[10] B. C. Bao, Z. Liu, and J. P. Xu, "Steady periodic memristor oscillator with transient chaotic behaviours," *Electronics Letters*, vol. 46, no. 3, pp. 228–230, 2010.

[11] M. Chen, J. J. Yu, Q. Yu, C. D. Li, and B. C. Bao, "A memristive diode bridge-based canonical Chua's circuit," *Entropy*, vol. 16, no. 12, pp. 6464–6476, 2014.

[12] Z.-J. Li and Y.-C. Zeng, "A memristor oscillator based on a twin-T network," *Chinese Physics B*, vol. 22, no. 4, Article ID 040502, 2013.

[13] B. Bao, Z. Ma, J. Xu, Z. Liu, and Q. Xu, "A simple memristor chaotic circuit with complex dynamics," *International Journal of Bifurcation and Chaos*, vol. 21, no. 9, pp. 2629–2645, 2011.

[14] G. M. Maggio, O. de Feo, and M. P. Kennedy, "Nonlinear analysis of the Colpitts oscillator and applications to design," *IEEE Transactions on Circuits and Systems I: Fundamental Theory and Applications*, vol. 46, no. 9, pp. 1118–1130, 1999.

[15] S.-M. Yu, "Fourth-order Colpitts chaotic oscillator," *Acta Physica Sinica*, vol. 57, no. 6, pp. 3374–3379, 2008 (Chinese).

[16] X. Y. Wang, A. L. Fitch, H. H. C. Iu, V. Sreeram, and W. G. Qi, "Implementation of an analogue model of a memristor based on a light-dependent resistor," *Chinese Physics B*, vol. 21, no. 10, Article ID 108501, 2012.

[17] X. Y. Wang, A. L. Fitch, H. H. C. Iu, and W. G. Qi, "Design of a memcapacitor emulator based on a memristor," *Physics Letters A*, vol. 376, no. 4, pp. 394–399, 2012.

[18] B. C. Bao, J. J. Yu, F. W. Hu, and Z. Liu, "Generalized memristor consisting of diode bridge with first order parallel RC filter," *International Journal of Bifurcation and Chaos*, vol. 24, no. 11, Article ID 1450143, 4 pages, 2014.

[19] F. Corinto and A. Ascoli, "Memristive diode bridge with LCR filter," *Electronics Letters*, vol. 48, no. 14, pp. 824–825, 2012.

[20] L. O. Chua, "The fourth element," *Proceedings of the IEEE*, vol. 100, no. 6, pp. 1920–1927, 2012.

[21] S. P. Adhikari, M. P. Sah, H. Kim, and L. O. Chua, "Three fingerprints of memristor," *IEEE Transactions on Circuits and Systems I: Regular Papers*, vol. 60, no. 11, pp. 3008–3021, 2013.